

## Polarization of $\Lambda^0$ and $\bar{\Lambda}^0$ inclusively produced by 610 GeV/c $\Sigma^-$ and 525 GeV/c proton beams

J.L. Sánchez-López,<sup>13</sup> K.D. Nelson,<sup>16, a</sup> J. Engelfried,<sup>13, b</sup> U. Akgun,<sup>16</sup> G. Alkhazov,<sup>11</sup> J. Amaro-Reyes,<sup>13</sup> A.G. Atamantchouk,<sup>11, c</sup> A.S. Ayan,<sup>16</sup> M.Y. Balatz,<sup>8, c</sup> A. Blanco-Covarrubias,<sup>13</sup> N.F. Bondar,<sup>11</sup> P.S. Cooper,<sup>5</sup> L.J. Dauwe,<sup>17</sup> G.V. Davidenko,<sup>8</sup> U. Dersch,<sup>9, d</sup> A.G. Dolgolenko,<sup>8</sup> G.B. Dzyubenko,<sup>8</sup> R. Edelstein,<sup>3</sup> L. Emediato,<sup>19</sup> A.M.F. Endler,<sup>4</sup> I. Eschrich,<sup>9, e</sup> C.O. Escobar,<sup>19, f</sup> N. Estrada,<sup>13</sup> A.V. Evdokimov,<sup>8</sup> I.S. Filimonov,<sup>10, c</sup> A. Flores-Castillo,<sup>13</sup> F.G. Garcia,<sup>19, 5</sup> M. Gaspero,<sup>18</sup> I. Giller,<sup>12</sup> V.L. Golovtsov,<sup>11</sup> P. Gouffon,<sup>19</sup> E. Gülmez,<sup>2</sup> He Kangling,<sup>7</sup> M. Iori,<sup>18</sup> S.Y. Jun,<sup>3</sup> M. Kaya,<sup>16, g</sup> J. Kilmer,<sup>5</sup> V.T. Kim,<sup>11</sup> L.M. Kochenda,<sup>11</sup> I. Konorov,<sup>9, h</sup> A.P. Kozhevnikov,<sup>6</sup> A.G. Krivshich,<sup>11</sup> H. Krüger,<sup>9, i</sup> M.A. Kubantsev,<sup>8</sup> V.P. Kubarovsky,<sup>6</sup> A.I. Kulyavtsev,<sup>3, 5</sup> N.P. Kuropatkin,<sup>11, 5</sup> V.F. Kurshetsov,<sup>6</sup> A. Kushnirenko,<sup>3, 6</sup> S. Kwan,<sup>5</sup> J. Lach,<sup>5</sup> A. Lamberto,<sup>20</sup> L.G. Landsberg,<sup>6, c</sup> I. Larin,<sup>8</sup> E.M. Leikin,<sup>10</sup> Li Yunshan,<sup>7</sup> M. Luksys,<sup>14</sup> T. Lungov,<sup>19</sup> V.P. Maleev,<sup>11</sup> D. Mao,<sup>3, j</sup> Mao Chensheng,<sup>7</sup> Mao Zhenlin,<sup>7</sup> P. Mathew,<sup>3, k</sup> M. Mattson,<sup>3</sup> V. Matveev,<sup>8</sup> E. McCliment,<sup>16</sup> M.A. Moinester,<sup>12</sup> V.V. Molchanov,<sup>6</sup> A. Morelos,<sup>13</sup> A.V. Nemitkin,<sup>10</sup> P.V. Neoustroev,<sup>11</sup> C. Newsom,<sup>16</sup> A.P. Nilov,<sup>8, c</sup> S.B. Nurushev,<sup>6</sup> A. Ocherashvili,<sup>12, l</sup> Y. Onel,<sup>16</sup> E. Ozel,<sup>16</sup> S. Ozkorucuklu,<sup>16, m</sup> A. Penzo,<sup>20</sup> S.V. Petrenko,<sup>6</sup> P. Pogodin,<sup>16, n</sup> M. Procaro,<sup>3, o</sup> V.A. Prutskoj,<sup>8</sup> E. Ramberg,<sup>5</sup> G.F. Rappazzo,<sup>20</sup> B.V. Razmyslovich,<sup>11, p</sup> V.I. Rud,<sup>10</sup> J. Russ,<sup>3</sup> P. Schiavon,<sup>20</sup> J. Simon,<sup>9, q</sup> A.I. Sitnikov,<sup>8</sup> D. Skow,<sup>5</sup> V.J. Smith,<sup>15</sup> M. Srivastava,<sup>19</sup> V. Steiner,<sup>12</sup> V. Stepanov,<sup>11, p</sup> L. Stutte,<sup>5</sup> M. Svoiski,<sup>11, p</sup> N.K. Terentyev,<sup>11, 3</sup> G.P. Thomas,<sup>1</sup> I. Torres,<sup>13</sup> L.N. Uvarov,<sup>11</sup> A.N. Vasiliev,<sup>6</sup> D.V. Vavilov,<sup>6</sup> E. Vázquez-Jáuregui,<sup>13</sup> V.S. Verebryusov,<sup>8</sup> V.A. Victorov,<sup>6</sup> V.E. Vishnyakov,<sup>8</sup> A.A. Vorobyov,<sup>11</sup> K. Vorwalter,<sup>9, r</sup> J. You,<sup>3, 5</sup> Zhao Wenheng,<sup>7</sup> Zheng Shuchen,<sup>7</sup> and R. Zukanovich-Funchal<sup>19</sup>

(The SELEX Collaboration)

<sup>1</sup>Ball State University, Muncie, IN 47306, U.S.A.

<sup>2</sup>Bogazici University, Bebek 80815 Istanbul, Turkey

<sup>3</sup>Carnegie-Mellon University, Pittsburgh, PA 15213, U.S.A.

<sup>4</sup>Centro Brasileiro de Pesquisas Físicas, Rio de Janeiro, Brazil

<sup>5</sup>Fermi National Accelerator Laboratory, Batavia, IL 60510, U.S.A.

<sup>6</sup>Institute for High Energy Physics, Protvino, Russia

<sup>7</sup>Institute of High Energy Physics, Beijing, P.R. China

<sup>8</sup>Institute of Theoretical and Experimental Physics, Moscow, Russia

<sup>9</sup>Max-Planck-Institut für Kernphysik, 69117 Heidelberg, Germany

<sup>10</sup>Moscow State University, Moscow, Russia

<sup>11</sup>Petersburg Nuclear Physics Institute, St. Petersburg, Russia

<sup>12</sup>Tel Aviv University, 69978 Ramat Aviv, Israel

<sup>13</sup>Universidad Autónoma de San Luis Potosí, San Luis Potosí, Mexico

<sup>14</sup>Universidade Federal da Paraíba, Paraíba, Brazil

<sup>15</sup>University of Bristol, Bristol BS8 1TL, United Kingdom

<sup>16</sup>University of Iowa, Iowa City, IA 52242, U.S.A.

<sup>17</sup>University of Michigan-Flint, Flint, MI 48502, U.S.A.

<sup>18</sup>University of Rome "La Sapienza" and INFN, Rome, Italy

<sup>19</sup>University of São Paulo, São Paulo, Brazil

<sup>20</sup>University of Trieste and INFN, Trieste, Italy

(Dated: June 23, 2007)

We have measured the polarization of  $\Lambda^0$  and  $\bar{\Lambda}^0$  inclusively produced by 610 GeV/c  $\Sigma^-$  and 525 GeV/c proton beams in the experiment SELEX during the 1996/7 fixed target run at Fermilab. The polarization was measured as a function of the  $\Lambda$  longitudinal momentum fraction  $x_F$  and transverse momentum  $p_t$ . For the  $\Lambda^0$  produced by  $\Sigma^-$  the polarization is increasing with  $x_F$ , from slightly negative at  $x_F \sim 0$  to about 15% at large  $x_F$ ; it shows a non-monotonic behavior as a function of  $p_t$ . For the proton beam, the  $\Lambda^0$  polarization is negative and decreasing as a function of  $x_F$  and  $p_t$ . The  $\bar{\Lambda}^0$  polarization is compatible with 0 for both beam particles over the full kinematic range. The target dependence was examined but no statistically significant difference was found.

## I. INTRODUCTION

A large number of theoretical models have been constructed over the years since it was first observed that inclusively produced hyperons are polarized. These models have met with varying degrees of success, but it is clear that more data and theoretical work are needed to clarify the picture. A review of the current status is found in [1–4].  $\Lambda$  polarization is well studied with a proton beam, both in inclusive [5] and exclusive [6–8] reactions. For  $\Sigma^-$  beam, only the WA89 experiment at CERN reports polarization measurements for  $\Lambda^0$  and  $\bar{\Lambda}^0$  as function of  $p_t$  for one average value of  $x_F$  [9], and for  $\Lambda^0$  as function of both  $p_t$  and  $x_F$  [10]. In the latter case the polarization is negative for small  $x_F$ , incrementing to positive values with  $x_F$ , but with a non-monotonic behavior as a function of  $p_t$  for different values of  $x_F$ .

In this study we exploit the capabilities of the SELEX apparatus to measure the polarization of  $\Lambda^0$  and  $\bar{\Lambda}^0$  inclusively produced by  $\Sigma^-$  and proton beams. The goal is to measure the polarizations as functions of  $x_F$  and  $p_t$  with higher beam momenta as the earlier WA89 measurement, using a different analysis method presenting different systematics, and extending the  $\Lambda^0$  polarization measurements to several values in  $x_F$ ; in addition, we add as a cross check the measurements with proton beam within the same experiment.

The SELEX (E781) experiment at Fermilab is a fixed target experiment designed primarily for high statistics studies of charmed baryons produced by a charged hyperon beam incident on a segmented copper/carbon target. However, the versatility of the apparatus allowed for the study of other reactions [11] in the same target. In this work we study the polarization of inclusively produced  $\Lambda^0$  and  $\bar{\Lambda}^0$ . More specifically we determine the po-

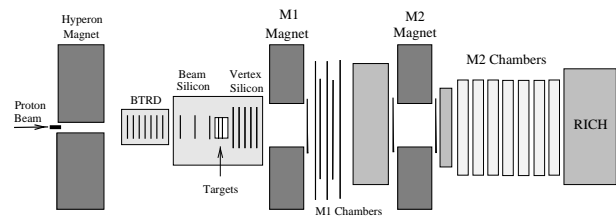


FIG. 1: Experimental apparatus for this analysis (not to scale).

larization and its  $x_F$  and  $p_t$  dependence. We follow the Basel Convention [12] for the sign of the polarization.

## II. EXPERIMENT

The charged hyperon beam, which we use as a primary beam for  $\Lambda$  production, was obtained in the Fermilab proton center beamline by steering 800 GeV/c protons from the Tevatron onto a 1 mm  $\times$  2 mm  $\times$  40 cm beryllium target located at the entrance of a 7.3 m, 3.5 T hyperon magnet [13]. A curved channel in this magnet selected a beam of negative (positive) particles with a mean momentum of 610 GeV/c (520 GeV/c) and a spread of  $\Delta p/p \approx 8\%$  HWHM. The negative beam consisted of approximately equal parts  $\Sigma^-$  and  $\pi^-$  with a small admixture of  $\Xi^-$  and  $K^-$ , while the positive beam contained about 92% protons, in a total of  $6 \times 10^5$  beam particles per second. The targeting angle was set to zero degrees, thereby insuring an unpolarized incident beam.

The portion of the experimental setup relevant to this analysis, which is shown in Fig. 1, consisted of a beam spectrometer, a vertexing region and two downstream spectrometers (M1 and M2). The beam spectrometer included the hyperon magnet, beam transition radiation detectors (BTRD) and beam silicon strip detectors (BSSD). The vertex region consisted of five segmented targets (2 Cu, 3 C each separated by 1.5 cm - altogether 5% of an interaction length) and 20 planes of vertex silicon strip detectors (VSSD), which resolved the interaction vertex and secondary vertices. For VSSD tracks, the transverse position resolution was  $4 \mu\text{m}$  at 600 GeV/c. The M1 spectrometer was a wide angle spectrometer, designed to analyze particles with momenta between  $\sim 2.5$  and  $\sim 15$  GeV/c. This spectrometer contained the M1 magnet ( $\Delta p_t = 0.74$  GeV/c), large angle silicon strip detectors (LASD), and proportional multi-wire chambers (PWC). The second spectrometer (M2), downstream of M1, analyzed particles with momenta  $\gtrsim 15$  GeV/c. Its components were the M2 magnet ( $\Delta p_t = 0.845$  GeV/c), LASD, PWC, and a ring-imaging Cherenkov (RICH) detector [14] used for particle identification, which provided  $\pi/p$  separation up to 330 GeV/c. A hardware trigger and software filter were used in SELEX to select the secondary interactions. The hardware trigger consisted of the beam, veto and hodoscope scintillation counters. The first level synchronized the trigger to beam parti-

<sup>a</sup>Present address: University of Alabama at Birmingham, Birmingham, AL 35294

<sup>b</sup>Electronic address: jurgen@ifisica.uaslp.mx

<sup>c</sup>deceased

<sup>d</sup>Present address: Advanced Mask Technology Center, Dresden, Germany

<sup>e</sup>Present address: University of California at Irvine, Irvine, CA 92697, USA

<sup>f</sup>Present address: Instituto de Física da Universidade Estadual de Campinas, UNICAMP, SP, Brazil

<sup>g</sup>Present address: Kafkas University, Kars, Turkey

<sup>h</sup>Present address: Physik-Department, Technische Universität München, 85748 Garching, Germany

<sup>i</sup>Present address: The Boston Consulting Group, München, Germany

<sup>j</sup>Present address: Lucent Technologies, Naperville, IL

<sup>k</sup>Present address: Baxter Healthcare, Round Lake IL

<sup>l</sup>Present address: NRCN, 84190 Beer-Sheva, Israel

<sup>m</sup>Present address: Süleyman Demirel Üniversitesi, Isparta, Turkey

<sup>n</sup>Present address: Legal Department, Oracle Corporation, Redwood Shores, California

<sup>o</sup>Present address: DOE, Germantown, MD

<sup>p</sup>Present address: Solidum, Ottawa, Ontario, Canada

<sup>q</sup>Present address: Siemens Medizintechnik, Erlangen, Germany

<sup>r</sup>Present address: Allianz Insurance Group IT, München, Germany

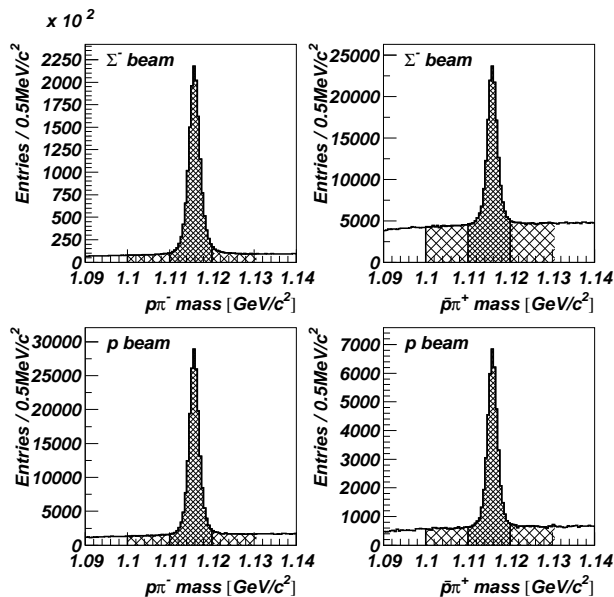


FIG. 2: Invariant mass distributions for  $p\pi^-$  (left) and  $\bar{p}\pi^+$  (right) for  $\Sigma^-$  (top) and proton (bottom) beams. The signal and sideband regions are indicated.

cles. The second level selected events where the BTRD determined the beam particle was most likely a heavy particles ( $\Sigma^-$  or proton), with an additional refined definition in the analysis stage. The beam interacted in one of the five targets, and more than 3 charged tracks were observed downstream of the target region of which at least 2 were positive tracks with momentum greater than  $\sim 15$  GeV/c. Triggered events accounted for 30% of interactions. A software filter looked for evidence of a secondary vertex and a reconstructed primary vertex using high momentum ( $\gtrsim 15$  GeV/c) tracks. The software filter further reduced the data set by a factor of 8. A sample of unfiltered data was always recorded for filter performance and systematic error analysis.

### III. DATA ANALYSIS

The  $\Lambda^0 \rightarrow p\pi^-$  ( $\bar{\Lambda}^0 \rightarrow \bar{p}\pi^+$ ) candidates were selected by requiring oppositely charge track pairs to form a vertex at least  $5\sigma$  downstream of the primary vertex, where  $\sigma$  is the combined error of the  $z$ -coordinates of the primary and secondary vertex, and upstream of the first VSSD plane. The positive (negative) track was required to be identified by the RICH as a proton candidate. In Fig. 2 we show the invariant mass distributions of these  $p\pi^-$  and  $\bar{p}\pi^+$  candidates, and in table I we summarize the available statistics. The  $K_S^0 \rightarrow \pi^+\pi^-$  decays are also included to be able to cross check the analysis procedure.

The polarization analysis consisted of extracting the polarization  $\mathbf{P}$  from a fit to the proton decay distribution

TABLE I: Number of  $\Lambda^0$ ,  $\bar{\Lambda}^0$  and  $K_S^0$  for the different beams.

Beam Particle	$\langle p \rangle$	# $\Lambda^0$	# $\bar{\Lambda}^0$	# $K_S^0$
$\Sigma^-$	611 GeV/c	1,360,000	112,000	4,698,000
$p$	525 GeV/c	162,000	35,700	752,000

in the  $\Lambda$  rest frame:

$$\frac{dN_{\text{meas}}}{d\cos\theta} \propto A(\cos\theta, x_F, p_t)[1 + \alpha_\Lambda \mathbf{P} \cos\theta] \quad (1)$$

where the  $y$ -axis is normal to the production plane (defined by the vector of the incoming beam particle and the outgoing  $\Lambda$ ), the  $z$ -axis is the direction of the  $\Lambda$  line-of-flight, and the  $x$ -axis completes the orthogonal triad.  $N_{\text{meas}}$  is the number of events,  $\theta$  is the angle between the proton line of flight and the coordinate axes,  $\alpha_\Lambda = 0.642 \pm 0.013$  is the asymmetry parameter [15], and  $A$  is the acceptance function. By parity conservation in the production process, the only polarization allowed is along the  $y$ -axis. Clearly, no polarization should be measured along the  $x$  or  $z$  direction.

Apparatus (or false) asymmetries are present along all axes. The false asymmetries can be removed by using a bias canceling technique, or by modeling the acceptance function  $A$  with Monte Carlo simulations. Bias canceling requires a subdivision of the available statistics, while the Monte Carlo simulation requires a good understanding of the apparatus and extensive computing time. Due to the overall low statistics compared to other measurements we present here results obtained [16] with the latter; however, with the bias canceling technique we obtained compatible results [17]. The analysis methods were validated by a non-observation of polarization in the forbidden projections, by analyzing the  $K_S^0$  with the same programs, and by Monte Carlo simulation via re-obtaining a known polarization.

To obtain the polarization of  $\Lambda^0$  produced by a  $\Sigma^-$  beam, we divided the data into 100 bins, 10 each in  $0.0 \leq x_F \leq 1.0$ , and in  $0.0 \text{ GeV}/c \leq p_t \leq 2.0 \text{ GeV}/c$ . The dependence of the acceptance function  $A$  on  $x_F$  and  $p_t$  can be neglected within one bin, and only the dependence on  $\cos\theta$  has to be taken into account. For each  $[x_F, p_t]$  bin a two-dimensional histogram of the cosine of the angle versus the invariant mass of the  $p\pi^-$  is filled and the  $dN_{\text{meas}}/d\cos\theta$  distribution is obtained via sideband subtraction (see also Fig. 2). To correct for the acceptance, we obtain the same distribution from Monte Carlo simulation (we verified that the acceptance is independent of an initial polarization of the Monte Carlo sample), and correct for the acceptance in each  $[x_F, p_t]$  bin separately. A straight line fit is performed to the final distribution, and the polarization is extracted according to equation 1.

For the lower statistics sample of  $\bar{\Lambda}^0$  and the proton beam data, it was not possible to subdivide the available data as before. Only measurements as a function of  $x_F$  and  $p_t$ , averaging over the other variable, could

TABLE II: Polarization (in %) of  $\Lambda^0$  inclusively produced by  $\Sigma^-$  as a function of  $x_F$  and  $p_t$ . The same information is shown in figures 3 and 4.

$x_F$	$\langle p_T \rangle$ [ GeV/c ]					
	0.1	0.3	0.5	0.7	0.9	1.1
0.15	$1.3 \pm 1.7$	$-0.5 \pm 1.2$	$-3.5 \pm 1.1$	$1.9 \pm 1.2$	$0.4 \pm 1.5$	$-1.6 \pm 1.9$
0.25	$0.4 \pm 2.0$	$-0.4 \pm 1.4$	$1.0 \pm 1.4$	$0.2 \pm 1.6$	$-1.0 \pm 1.9$	$-0.8 \pm 2.6$
0.35	$3.5 \pm 2.6$	$-0.6 \pm 1.8$	$1.7 \pm 1.8$	$7.5 \pm 1.9$	$4.7 \pm 2.4$	$0.7 \pm 3.3$
0.45	$2.6 \pm 3.4$	$8.1 \pm 2.3$	$9.9 \pm 2.3$	$6.4 \pm 2.5$	$6.6 \pm 3.0$	$10.8 \pm 4.2$
0.55	$5.4 \pm 5.2$	$5.4 \pm 3.3$	$10.5 \pm 3.2$	$12.6 \pm 3.4$	$10.0 \pm 4.2$	$6.3 \pm 5.7$
0.65	$7.0 \pm 7.7$	$5.4 \pm 4.7$	$22.6 \pm 4.7$	$16.4 \pm 5.4$	$11.2 \pm 6.4$	$21.4 \pm 8.8$
0.75	$-8.5 \pm 10.3$	$11.8 \pm 7.3$	$13.6 \pm 7.5$	$13.0 \pm 9.3$	$-9 \pm 13$	$5 \pm 17$
0.85	$25 \pm 19$	$16 \pm 14$	$11 \pm 16$	$41 \pm 22$	$10 \pm 25$	$56 \pm 53$

be performed. As described above, a two-dimensional histogram was filled, but this time with a weight factor obtained from an acceptance model which takes into account the  $x_F$ ,  $p_t$  as well as the primary interaction target dependence of the acceptance [18].

#### IV. SYSTEMATIC CHECKS

We performed several systematic checks to verify our analysis method, including the algorithm as well as the acceptance model. We analysed simulated samples of known polarization, and always re-obtained the correct result. We observed asymmetries in forbidden projections compatible with 0. We also measured the asymmetry of  $K_S^0 \rightarrow \pi^+\pi^-$  decays which again is compatible with 0 over the full kinematic range as shown in the last columns of tables III and IV.

Other systematic checks included harder cuts on the separation between primary vertex and  $\Lambda$  decay vertex, requiring that also the pion track reaches the M2 spectrometer, and that the pion is identified with the RICH detector. We always obtained, within the statistical errors, the same results for all polarizations. For these reasons we only quote statistical errors on all our measurements.

#### V. RESULTS

In Figs. 3 and 4, as well as in table II we present our results for the  $\Lambda^0$  polarization with a  $\Sigma^-$  beam as function of  $x_F$  and  $p_t$ .

Figure 5 shows the polarization of  $\Lambda^0$  and  $\bar{\Lambda}^0$  produced by  $\Sigma^-$  and protons. Due to the lower statistics available, only the distributions for an average value of  $x_F$  and  $p_t$  are shown. The same information is presented in tables III and IV.

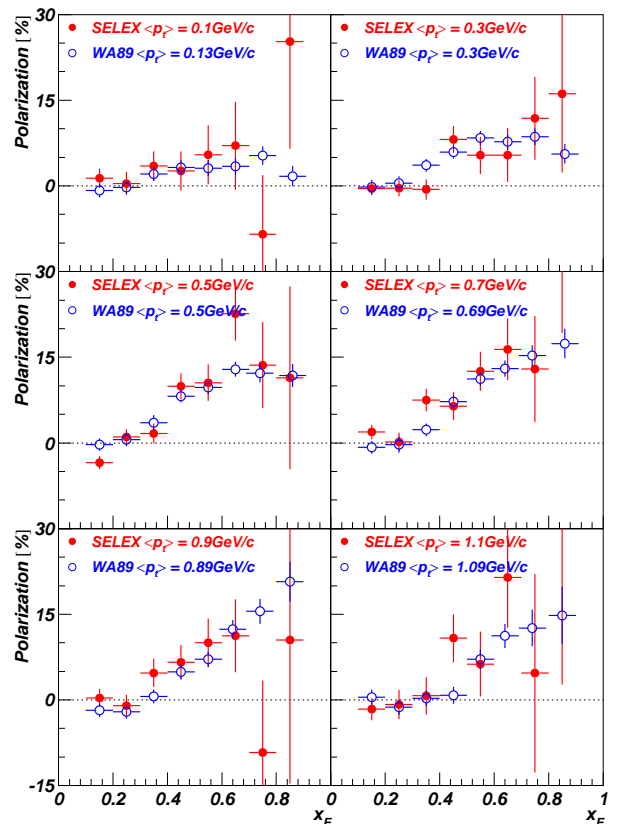


FIG. 3: Polarization of  $\Lambda^0$  inclusively produced by  $\Sigma^-$  as a function of  $x_F$  for different  $p_t$  values. Also shown are data from ref. [10]. The SELEX data points are also given in table II.

#### VI. DISCUSSION AND CONCLUSIONS

For the inclusive production of  $\Lambda^0$  by a  $\Sigma^-$  beam, our results confirm the WA89 [9, 10] measurements (obtained via the bias canceling method) of a generally positive polarization, increasing with  $x_F$ , as shown in Fig. 3 and 4. At small  $p_t$  and  $x_f$  the polarization is almost 0, and in general the dependence on  $p_t$  is non-monotonic for different bins of  $x_F$ , increasing and decreasing after reaching some maximum value. Comparing to the earlier, lower-

TABLE III: Polarization (in %) of  $\Lambda^0$  and  $\overline{\Lambda^0}$  produced by  $\Sigma^-$  and protons, as function of  $p_t$ , averaged over  $x_F$ . The same information is presented graphically in Fig. 5 (left). Also shown are the asymmetry values measured for the  $K_S^0$ .

$p_t$ [GeV/c]	$pN \rightarrow \Lambda^0 X$ $\langle x_F \rangle = 0.24$	$pN \rightarrow \overline{\Lambda^0} X$ $\langle x_F \rangle = 0.11$	$\Sigma^- N \rightarrow \overline{\Lambda^0} X$ $\langle x_F \rangle = 0.11$	$\Sigma^- N \rightarrow \Lambda^0 X$ $\langle x_F \rangle = 0.29$	$\Sigma^- N \rightarrow K_S^0 X$ Asymmetry
0.1	–	–	–	$0.1 \pm 0.9$	$-0.1 \pm 0.4$
0.3	$-2.9 \pm 1.9$	$-1.0 \pm 3.9$	$2.8 \pm 2.8$	$2.7 \pm 0.6$	$0.6 \pm 0.3$
0.5	$-6.6 \pm 1.8$	$-7.3 \pm 3.6$	$2.5 \pm 2.4$	$4.0 \pm 0.6$	$-0.1 \pm 0.3$
0.7	$-3.7 \pm 2.0$	$-6.0 \pm 3.9$	$-0.9 \pm 2.6$	$5.7 \pm 0.7$	$0.3 \pm 0.4$
0.9	$-5.9 \pm 2.6$	$0.8 \pm 5.4$	$-1.5 \pm 3.3$	$1.4 \pm 0.9$	$0.6 \pm 0.5$
1.1	$-12.4 \pm 3.7$	$15.8 \pm 8.2$	$0.7 \pm 4.9$	$4.2 \pm 1.2$	$-1.0 \pm 0.7$
1.3	$-9.2 \pm 5.4$	$14.3 \pm 13.3$	$0.4 \pm 7.2$	$-0.3 \pm 1.7$	$0.3 \pm 1.0$
1.5	–	–	–	$-6.6 \pm 2.5$	$0.6 \pm 1.5$
1.7	–	–	–	$0.3 \pm 3.9$	$-2.1 \pm 2.3$
1.9	–	–	–	$1.9 \pm 5.8$	$-2.8 \pm 3.5$

TABLE IV: Polarization (in %) of  $\Lambda^0$  and  $\overline{\Lambda^0}$  produced by  $\Sigma^-$  and protons, as function of  $x_F$ , averaged over  $p_t$ . The same information is presented graphically in Fig. 5 (right). Also shown are the asymmetry values measured for the  $K_S^0$ .

$\langle p_t \rangle$	$pN \rightarrow \Lambda^0 X$ 0.59 GeV/c	$pN \rightarrow \overline{\Lambda^0} X$ 0.60 GeV/c	$\Sigma^- N \rightarrow \overline{\Lambda^0} X$ 0.63 GeV/c	$\Sigma^- N \rightarrow \Lambda^0 X$ 0.57 GeV/c	$\Sigma^- N \rightarrow K_S^0 X$ Asymmetry
0.05	–	–	–	$0.6 \pm 0.6$	$0.4 \pm 0.2$
0.15	$-3.8 \pm 1.5$	$-3.3 \pm 3.0$	$1.7 \pm 2.2$	$-0.2 \pm 0.5$	$0.0 \pm 0.3$
0.25	$-6.4 \pm 2.1$	$-0.7 \pm 6.4$	$-5.4 \pm 4.3$	$-1.0 \pm 0.7$	$-0.3 \pm 0.5$
0.35	$-7.2 \pm 3.1$	$42 \pm 15$	$0 \pm 14$	$3.3 \pm 0.8$	$-0.4 \pm 1.0$
0.45	$-1.7 \pm 4.4$	$-23 \pm 36$	$-29 \pm 50$	$7.8 \pm 1.1$	$1.4 \pm 2.3$
0.55	$-5.0 \pm 6.3$	–	$25 \pm 61$	$7.2 \pm 1.6$	$-4.4 \pm 5.2$
0.65	$-7.3 \pm 9.2$	–	–	$14.2 \pm 2.4$	$7 \pm 14$
0.75	–	–	–	$10.1 \pm 3.9$	$48 \pm 46$
0.85	–	–	–	$16.9 \pm 8.2$	–
0.95	–	–	–	$-15 \pm 30$	–

statistics WA89 [9] result with the dependence on  $p_t$  for  $\langle x_F \rangle = 0.30$  (Fig. 5, upper left and table III), we observe small polarization values confirming the previous measurement. The authors of [10] attribute the non-monotonic behavior of the polarization as function of  $p_t$  and  $x_F$  to different production mechanism in different kinematic regimes. We also examined the target dependence, but no difference was found.

For the polarization for  $\Lambda^0$  produced by a proton beam as a function of  $p_t$ , our results coincide with the higher statistics, but lower beam momentum, results from E008 [5]. In Fig. 5 (upper right) and table IV we also present polarization results as a function of  $x_F$  and compare them to our  $\Sigma^-$  data.

The  $\overline{\Lambda^0}$  polarization is compatible with 0, for  $\Sigma^-$  and proton beams for all  $p_t$  values measured, as obtained in [5, 9]. In addition we present also the polarization as function of  $x_F$  (Fig. 5 (lower right) and table IV).

In conclusion, we measured the polarization of inclusively produced  $\Lambda^0$  with a  $\Sigma^-$  beam, and confirming the WA89 results with a different analysis method and higher beam momentum. We do not observe any polarization of the  $\overline{\Lambda^0}$  at  $p_t \leq 1.3$  GeV/c and  $x_F \leq 0.55$ . The  $\Lambda^0$  polarization with a proton beam is compatible with earlier results.

## Acknowledgments

The authors are indebted to the staff of Fermi National Accelerator Laboratory and for invaluable technical support from the staffs of collaborating institutions. This project was supported in part by Bundesministerium für Bildung, Wissenschaft, Forschung und Technologie, Consejo Nacional de Ciencia y Tecnología (CONACyT), the Secretaría de Educación Pública (Mexico) (grant number 2003-24-001-026), Fondo de Apoyo a la Investigación (UASLP), Conselho Nacional de Desenvolvimento Científico e Tecnológico, Fundação de Amparo à Pesquisa do Estado de São Paulo (FAPESP), the Israel Science Foundation founded by the Israel Academy of Sciences and Humanities, Istituto Nazionale di Fisica Nucleare (INFN), the International Science Foundation (ISF), the National Science Foundation (Phy #9602178), NATO (grant CR6.941058-1360/94), the Russian Academy of Science, the Russian Ministry of Science and Technology, the Russian Foundation for Basic Research (RFBR grant 05-02-17869), the Turkish Scientific and Technological Research Board (TÜBİTAK), and the U.S. Department of Energy (DOE grant DE-FG02-91ER40664 and DOE contract number DE-AC02-76CHO3000).

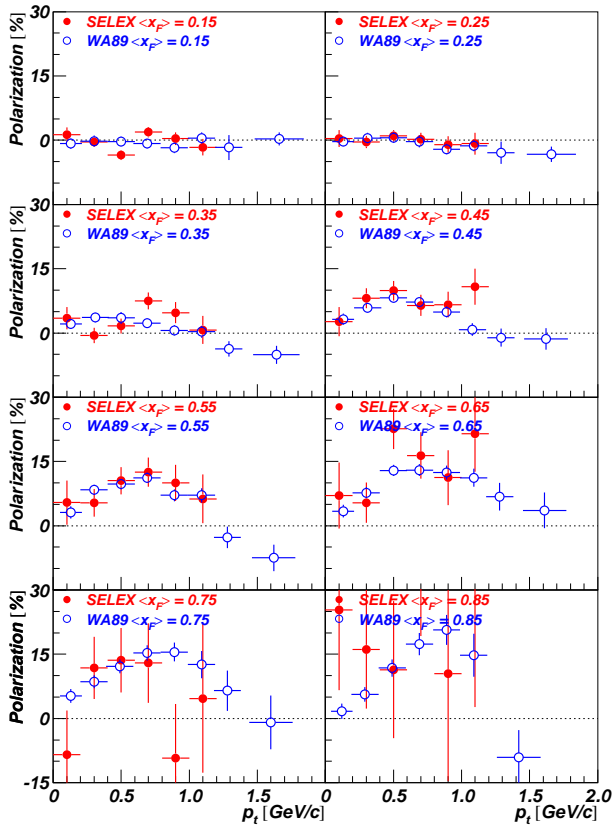


FIG. 4: Polarization of  $\Lambda^0$  inclusively produced by  $\Sigma^-$  as a function of  $p_t$  for different  $x_F$  values. Also shown are data from ref. [10]. The SELEX data points are also given in table II.

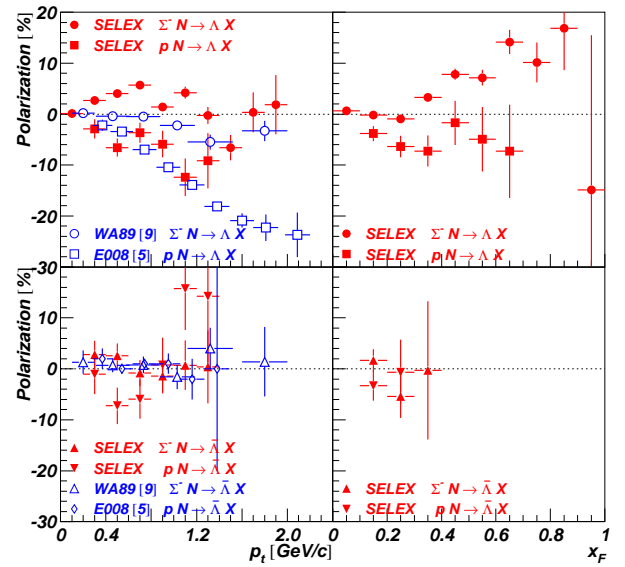


FIG. 5: Polarization of  $\Lambda^0$  (top) and  $\bar{\Lambda}^0$  (bottom) produced by  $\Sigma^-$  and protons, as function of  $p_t$  (left) and  $x_F$  (right). Also shown are data from Refs. [5, 9]. The SELEX data points are also given in tables III and IV.

- [1] J. Lach, Nucl. Phys. Proc. Suppl. **50**, 216 (1996).
- [2] J. Felix, Mod. Phys. Lett. A **12**, 363 (1997).
- [3] J. Felix, Mod. Phys. Lett. A **14**, 827 (1999).
- [4] J. Felix, Mod. Phys. Lett. A **16**, 1741 (2001).
- [5] K. J. Heller *et al.*, Phys. Rev. Lett. **41**, 607 (1978) [Erratum-ibid. **45**, 1043 (1980)].
- [6] J. Felix *et al.*, Phys. Rev. Lett. **76**, 22 (1996).
- [7] J. Felix *et al.*, Phys. Rev. Lett. **82**, 5213 (1999).
- [8] J. Felix *et al.* [E690 Collaboration], Phys. Rev. Lett. **88**, 061801 (2002).
- [9] M. I. Adamovich *et al.* [WA89 Collaboration], Z. Phys. A **350**, 379 (1995) [arXiv:hep-ex/9409001].
- [10] M. I. Adamovich *et al.* [WA89 Collaboration], Eur. Phys. J. C **32**, 221 (2004).
- [11] P. Pogodin *et al.* [SELEX Collaboration], Phys. Rev. D **70**, 112005 (2004).
- [12] V.W. Hughes *et al.*, “last page”, Proceedings of the International Symposium on Polarization Phenomena of Nucleons, Basel, Switzerland, July 1960.
- [13] J. Lach, “E781 hyperon beam and targeting system,” FERMILAB-TM-2129 (2000).
- [14] J. Engelfried *et al.*, Nucl. Instrum. Meth. A **431**, 53 (1999) [arXiv:hep-ex/9811001].
- [15] W. M. Yao *et al.* [Particle Data Group], J. Phys. G **33**, 1 (2006).
- [16] J. L. Sanchez-Lopez, Master Thesis, Instituto de Física, Universidad Autónoma de San Luis Potosí, 2006. FERMILAB-MASTERS-2006-06.
- [17] K. D. Nelson, Ph.D. Thesis, University of Iowa, 1999. FERMILAB-THESIS-1999-55.
- [18] J. Engelfried, E. A. Blanco, J. L. Sanchez, SELEX Internal Note H-866 (2006).